引用格式：SUN Gaofei, MING Shanchi, ZHANG Guoyu, et al. Correction Method of Star Position Error for Splicing Star Simulator[J]. Acta Photonica Sinica, 2021, 50(9):0912006
孙高飞,明杉炽,张国玉,等.拼接星模拟器星位置误差校正方法[J].光子学报,2021,50(9):0912006

拼接星模拟器星位置误差校正方法

孙高飞,明杉炽,张国玉,刘石,徐达
(长春理工大学 光电工程学院吉林省光电测控仪器工程技术研究中心,长春 130022)

摘　要:为了提高拼接式星模拟器的星图模拟精度,克服传统方法仅通过修正主距提高精度的局限性,提出了一种星图模拟精度的像差校正方法。分析拼接式星模拟器的工作原理和使用方法,优化小畸变平像场高成像质量准直光学系统像差,并根据像差设计结果,结合星点位置测量模型,分别建立畸变修正模型、彗差、场曲的修正模型。利用经纬仪、六维调整机构搭建星点位置精度测量装置,实测结果表明:基于像差理论的修正模型可有效提高拼接式星模拟器的星图精度,最大星点位置误差从48.78″降低至10.75″,满足了技术指标。

关键词:星模拟器;星图模拟;像差;修正模型;星点位置精度
中图分类号:V524.7;TH74　　**文献标识码**:A　　**doi**:10.3788/gzxb20215009.0912006

Correction Method of Star Position Error for Splicing Star Simulator

SUN Gaofei, MING Shanchi, ZHANG Guoyu, LIU Shi, XU Da
(*Jilin Province Engineering Research Center*, *Jilin Province Engineering Research Center*, *College of Optoelectronic Engineering*, *Changchun University of Science and Technology*, *Changchun* 130022, *China*)

Abstract: A correction method is proposed to improve the star map simulation accuracy of splicing star simulator, which overcomes the limitation of conventional methods in improving star map accuracy merely through correcting the principal distance. The aberration of a small distortion flat field high imaging quality collimating optical system is optimized after analyzing the working principle and usage of splicing star simulator. Based on aberration design results and the star position measurement model, the correction models for distortion, coma, curvature of field are created separately. In addition, a device for measuring star position accuracy is built by utilizing the theodolite and six-dimensional adjustment mechanism. According to measurement results, the correction model based on aberration theorise effective in improving the star map accuracy of splicing star simulator. The maximum star position errorr educes from 48.78″ down to 10.75″, meetting the technical requirements.

Key words: Star simulator; Star map simulation; Aberration; Correction model; Star position error
OCIS Codes: 120.4800; 220.1000; 220.2740; 120.4800; 080.2740

0 Introduction

From the successful docking of Shenzhou XI with Tiangong 2 to the successful launch of Long March 5, the star sensor bothplays a decisive role in its stable operation in orbit. The precision of star point position is significant to identify the star map and to acquire the aircraft attitude for star sensors [1]. Star simulator, as

Foundation item: National Natural Science Foundation of China (No.61703057)
First author: SUN Gaofei (1985—), female, associate professor, PhD. degree, mainly focuses on space ground simulation test and calibration technology. Email:sungf@cust.edu.cn
Received: Mar. 9, 2021; **Accepted**: Jun. 9, 2021

essential equipment in ground test of star sensor, can effectively ensure in-orbit attitude measurement and control of satellite and spacecraft[2-3]. The accuracy of star simulator influences the development of star sensor[4-8].

Star point position, as the main indicator in the evaluation of the precision of star simulator, directly determines the angle precision of star simulator. In order to improve the star position accuracy, the star position should be corrected according to the design and installation results.The traditional correction method regards the different focal lengths of stars at different positions of the system as the reason for all errors. On the basis of multiple measurements, the focal length corresponding to each star point is determined, and then the new focal length is obtained based on the objective of minimizing the error, and then the corrected position of each star point under this focal length is deduced. For example, WANG Lingyun, et al corrected the star position error of Thin Film Transistor Liquid Crystal Display (TFT-LCD) star simulator, and the accuracy was better than 35"[9]. Due to the strong subjectivity of the test process[10] and the high contingency of multi-point test, it is unable to ensure the consistency of horizontal and pitching tests at the same time, resulting in some starlight output accuracy exceeding. In order to enhance the objectivity of the correction, through the analysis of the aberration of the optical system, the contribution of each aberration to the pixel offset is clarified. The comprehensive influence of the aberration is corrected, and the iterative focusing method can improve the starlight output accuracy of the system. XU Da et al, established a star position error correction model based on the wave aberration, realizing the precision of star point position higher than 10"[11]. Compared with the traditional TFT-LCD and Digital Micromirror Device (DMD) display chips, Liquid Crystal on Silicon (LCOS) has the advantages of high opening rate and small pixel size, so it can enhance the simulation range of star simulator and improve the accuracy of star position. ASTRIUM takes the lead in using LCOS as the display device of dynamic star simulator and realizes the high precision dynamic star simulator design[12]. The star diagonal error is less than 18". Because it is difficult to meet the design requirements of large field of view and high precision star simulator for single chip display, optical stitching technology is usually considered to effectively expand the effective size of image plane[13-15].

To this end, this study investigated the double-chip LCOS splicing star simulator and analyzed the lateral aberration theory of high precision imaging of star point position. An optical system with high imaging quality was designed. Moreover, the correction method was proposed, and a measurement model of star point position was established, expecting to provide a new idea and approach for improving the precision of star simulator.

1 Working principle

Two pieces of LCOS were spliced to realize a large field of view star simulation. The splicing star simulator consists LCOS 1, LCOS 2, Polarization Beam Splitter (PBS), small field angle light source, collimating optical system, star image display and control computer, which form a large field star map simulator. A starlight exit precision detection device composed of array CCD, its image acquisition system and

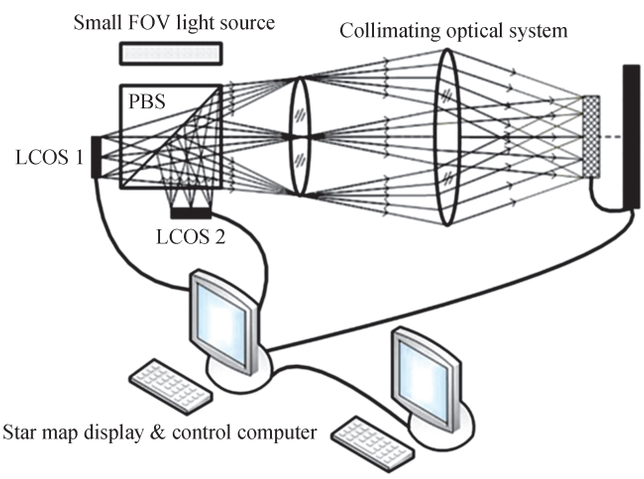

Fig.1 Experimental device diagram

high precision theodolite was used to further enhance the simulation precision of star point position. The star map information was received, and the closed loop detection and correction were implemented combined with the star map display and the control computer, as shown in Fig.1.

The star map display and the control computer generate the star map data observed by the star sensor according to the orientation of the coordinate axis of the star sensor in the inertial coordinate system, and the star map is generated on LCOS 1 and LCOS 2. The LCOS 1 and LCOS 2 are combined to form a mosaic image by the action of PBS, and the stars displayed in the image become parallel light after the collimation optical system, so as to realize the simulation of star map under laboratory conditions for the observation of star sensor. The indicators of the splicing star simulator are shown in Table 1.

Table 1 Star simulation indicators

Technical specifications	Index parameter
FOV	22°
Caliber	10 mm
Single star field angle	35″

2 Star simulator optical system based on lateral aberration

2.1 Lateral aberration theory

The aberration of optical system is divided into monochromatic aberration and chromatic aberration. There are various aberrations in the collimating optical system of star simulator, thereby influencing the imaging position and imaging quality of star points[16]. This section mainly analyzes the influence of distortion, coma and field curvature on lateral position deviation of image points through characteristic curve of aberration, as shown in Fig.2.

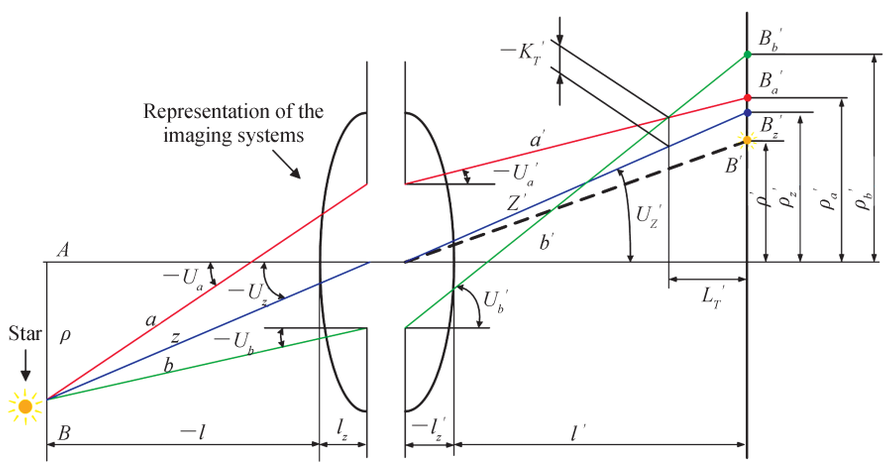

Fig.2 Influence of lateral aberration on off-axis imaging beams

1) Influence of distortion on star point position

Distortion is the monochromatic aberration caused by the change of optical system magnification with the angle between the beam and the principal axis. For star simulator, the distortion of collimating optical system only influences the imaging position of star. The aberration is calculated by Eqs. (1)~(3).

$$\rho=\sqrt{x'^2+y'^2} \tag{1}$$

$$\delta\rho_z'=\rho_z'-\rho \tag{2}$$

$$(x',y')=x+\delta\rho_z'\cos\left(\arctan\frac{y}{x}\right),y+\delta\rho_z'\sin\left(\arctan\frac{y}{x}\right) \tag{3}$$

where ρ is the distance between the star point and the center point in ideal situation. ρ_z' is the distance from the intersection point of the chiefray emitted from the off-axis point passing the optical system and the Gauss image

plane to the central point. $\delta\rho'_z$ is the centripetal offset caused by distortion.(x, y) is the position of ideal point; (x', y') is the actual distorted image position, which is expressed by Eq. (3).

2) Influence of coma on star point position

Coma is the asymmetry of off-axis ray of star point passing through the optical system, including the meridional coma and the sagittal coma. The meridional coma difference is three times that of the sagittal coma. The meridian coma is calculated by Eqs. (4)~(5).

$$K'_T = \frac{1}{2}(\rho'_a + \rho'_b) - \rho'_z \tag{4}$$

$$(x', y') = x + K'_T \cos\left(\arctan\frac{y}{x}\right), y + K'_T \sin\left(\arctan\frac{y}{x}\right) \tag{5}$$

where ρ'_a and ρ'_b are the distance from the intersection point of the upper and lower ray of the off-axis chief ray and the Gauss image plane to the central point. As shown in Fig.2, K'_T is the centripetal offset caused by the meridional coma. Eq. (5) represents the position (x', y') of image point.

3) Influence of field curvature on star point position

Field curvature indicates that the meridional and sagittal off-axis light beams of the star point cannot focus on a point after the action of the optical system. The meridional image points do not coincide with the sagittal image points, that is, the center and edge of the star cannot be clear simultaneously. The calculation of the field curvature is shown in Eqs. (6)~(8).

$$L'_T = \frac{\Delta\rho'_a - \Delta\rho'_b}{\tan U'_a - \tan U'_b} \tag{6}$$

$$\frac{l' - l'_z}{\rho'_z} = \frac{l' - l'_z - L'_T}{\rho'_T} \tag{7}$$

$$(x', y') = x + \delta\rho'_T \cos\left(\arctan\frac{y}{x}\right), y + \delta\rho'_T \sin\left(\arctan\frac{y}{x}\right) \tag{8}$$

where l' and l'_z have been marked in Fig.2. ρ'_T is the centripetal offset caused by field curvatureL'_T. $\delta\rho'_T$ is the difference between ρ'_T and ρ'. The actual image point position (x', y') is expressed by Eq. (8).

2.2 Evaluation of optimization parameters of collimating optical system

According to requirements for the field of view, aperture, single star angle and single star position precision of the splicing star simulator, combined with the influence of lateral aberration on imaging position and, a small distortion flat field high imaging quality collimating optical system was designed by ZEMAX. The optical structure is shown in Fig.3 and the aberration curve is shown in Fig.4.

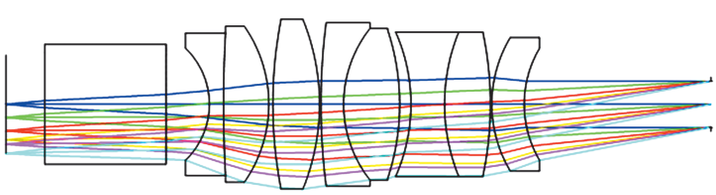

Fig.3 Optical structure

According to the aberration design results, when the Nyquist frequency is v=60 lp/mm, the design of the full field of view is better than 0.3. Both the field curvature and distortion are less than 0.2%, and the chromatic aberration of the maximum field of view is less than that of the Airy spot. The wavefront aberration of the edge field is 0.06 λ, which is better than the aberration tolerance of the Rayleigh criterion. The splicing star simulator evaluates the energy of the star point through the transmission of diffraction energy and system energy of the image points. Therefore, the enveloping circle energy and relative energy are designed as shown in Fig.5.

The energy images shows that when the point image radius is less than 50 μm, the percentage of point energy concentration is higher than 90%, and the relative energy changes slightly with the field of view. The brightness of the stars in the full field of view does not decrease in the imaging process of the optical system.

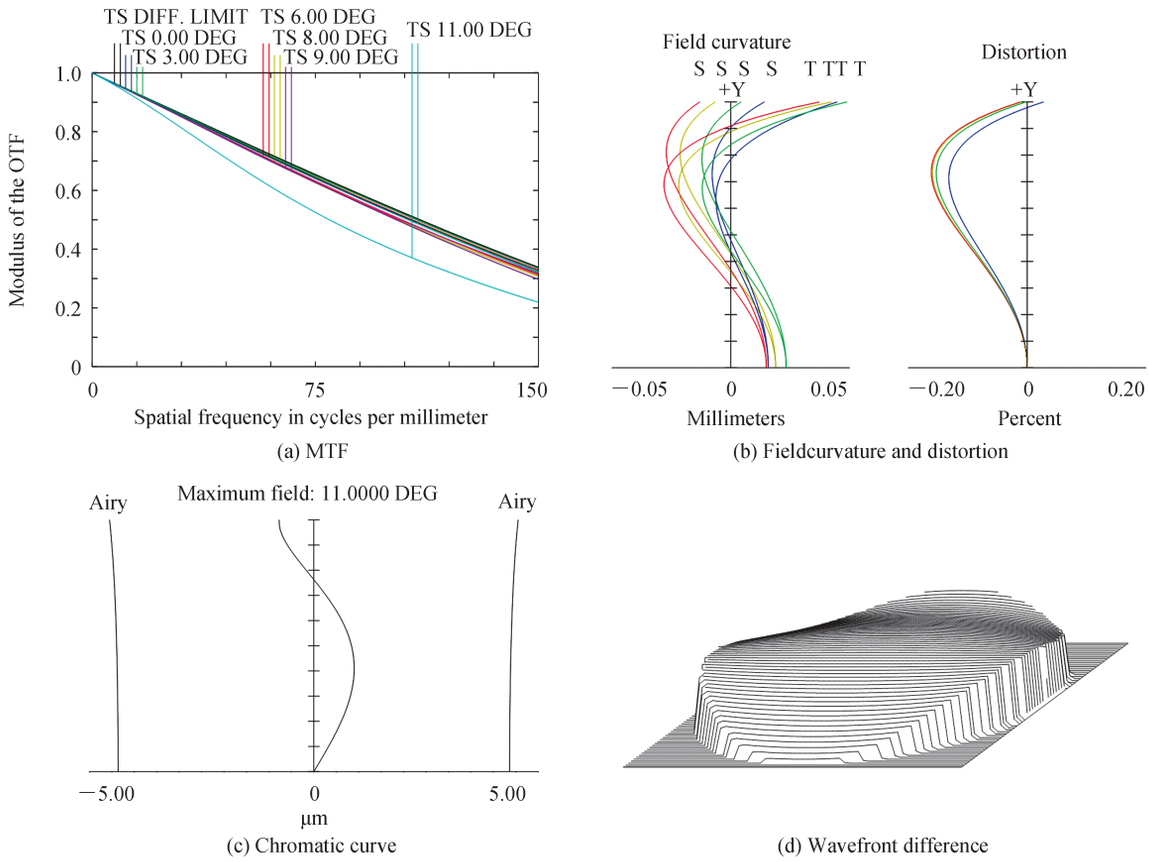

Fig.4 Aberrations of collimating optical system

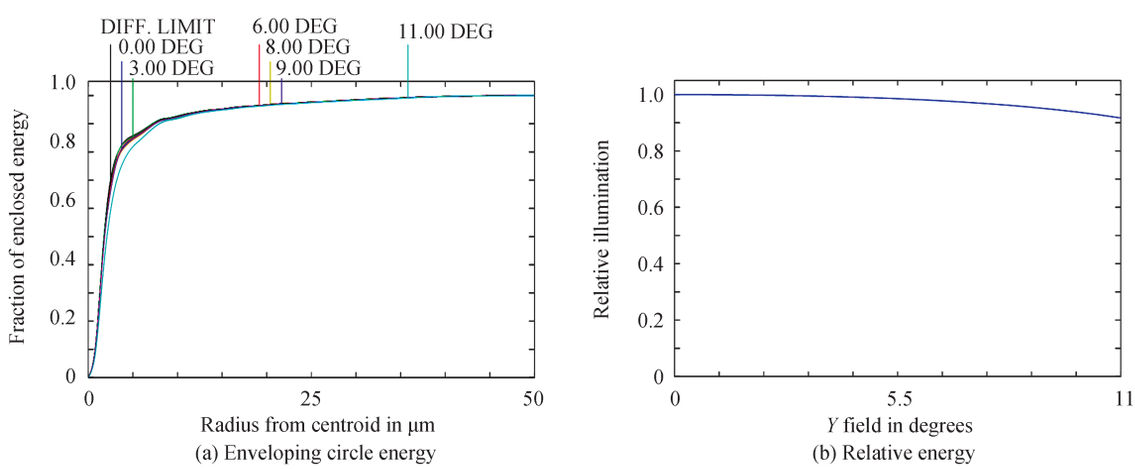

Fig.5 Energy images

3 Measurement model and correction method

3.1 Evaluation of optimization parameters of collimating optical system

The star position precision of star simulator includes single star position precision and star pair position precision. Single star position error refers to the relative position error of all star points relative to the central star point, while the star pair position error is the relative position error between any two star points. When one star of the star pair is the central star point, the star pair position error is the single star position error.

Considering the star position error measurement of splicing star simulator, the star display device LCOS is assumed to be placed on the focal plane and perpendicular to the optical axis of the optical system. According to the imaging principle of the splicing star simulator, the star position measurement model is shown in Fig.6.

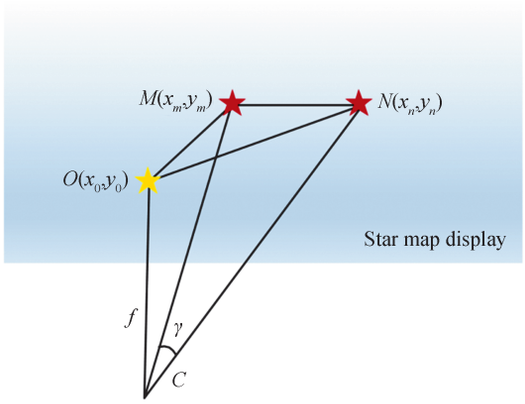

Fig.6 Star point measurement schematic map

Where, M and N are two stars on the star map display of the splicing star simulator. O is the central star. C is the test point of the star pair position. According to the star map recognition algorithm of star sensor[17], γ is the angular distance between stars, which is calculated by Eq. (9).

$$\gamma = \arctan\frac{\sqrt{\left(x_m - x_n\right)^2 + \left(y_m - y_n\right)^2}}{f} \tag{9}$$

where, f is the focal length of the optical system. $\left(x_m, y_m\right)$ is the position coordinates of arbitrary star point M. $\left(x_n, y_n\right)$ is the position coordinates of arbitrary star point N.

3.2 Correction method for star position error

The star position deviation caused by lateral aberration affects the image quality of collimating optical system. Although distortion does not influence the image definition of star point, it causes position deviation. Field curvature and coma prevent the star point beam from focusing on one point, thereby leading to unclear star imaging and speckle.The correction of star position in image plane under distortion, coma and field curvature is expressed by Eqs. (10)～(12), respectively.

$$\begin{cases}\Delta x_{i,\,\text{distortion}} = (\rho'_{zi} - \rho_i)\cos\left(\arctan\dfrac{y_i}{x_i}\right)\\ \Delta y_{i,\,\text{distortion}} = (\rho'_{zi} - \rho_i)\sin\left(\arctan\dfrac{y_i}{x_i}\right)\end{cases} \tag{10}$$

$$\begin{cases}\Delta x_{i,\,\text{coma}} = \left[\dfrac{1}{2}(\rho'_i + \rho'_i) - \rho'_i\right]\cos\left(\arctan\dfrac{y_i}{x_i}\right)\\ \Delta y_{i,\,\text{coma}} = \left[\dfrac{1}{2}(\rho'_{ai} + \rho'_{bi}) - \rho'_{zi}\right]\sin\left(\arctan\dfrac{y_i}{x_i}\right)\end{cases} \tag{11}$$

$$\begin{cases}\Delta x_{i,\,\text{field}} = \left[\rho'_{zi} - \rho_i - \dfrac{\rho'_{zi}(\Delta\rho'_{ai} - \Delta\rho'_{bi})}{(\tan U'_{ai} - \tan U'_{bi})(l_i - l'_{zi})}\right]\cos\left(\arctan\dfrac{y_i}{x_i}\right)\\ \Delta y_{i,\,\text{field}} = \left[\rho'_{zi} - \rho_i - \dfrac{\rho'_{zi}(\Delta\rho'_{ai} - \Delta\rho'_{bi})}{(\tan U'_{ai} - \tan U'_{bi})(l_i - l'_{zi})}\right]\sin\left(\arctan\dfrac{y_i}{x_i}\right)\end{cases} \tag{12}$$

where, $(\Delta x_{i,\,\text{distortion}}, \Delta y_{i,\,\text{distortion}})$ is the correction caused by distortion. ρ'_{zi} is the distance from the intersection point of the chiefray emitted from the star point passing the optical system and the Gauss image plane to the central point. $(\Delta x_{i,\,\text{coma}}, \Delta y_{i,\,\text{coma}})$ is the correction caused by coma. ρ_i is the distance between the star and the center in an ideal situation. $(\Delta x_{i,\,\text{field}}, \Delta y_{i,\,\text{field}})$ is the correction caused by field curvature. ρ'_{ai} and ρ'_{bi} are the distance from the intersection point of the upper and lower beams symmetrical at the off-axis chief ray and the Gauss image plane to the central point respectively.

However, the displacement of the star point, and the unclear image are caused by aberrations such as distortion, coma and field curvature. Therefore, the correction of the star point position on the image plane

should be represented by compound correction $(\Delta X_i, \Delta Y_i)$ under the influence of aberration, as shown in Eq. (13).

$$\begin{cases} \Delta X_i = \kappa_{\text{distortion}}\xi_{\text{distortion}}h_i^3\cos\phi_i + \kappa_{\text{coma}}\xi_{\text{coma}}u_i^2h_i\cos\phi_i + \kappa_{\text{field}}\xi_{\text{field}}u_ih_i^2\cos\phi_i \\ \Delta Y_i = \kappa_{\text{distortion}}\xi_{\text{distortion}}h_i^3\sin\phi_i + \kappa_{\text{coma}}\xi_{\text{coma}}u_i^2h_i\sin\phi_i + \kappa_{\text{field}}\xi_{\text{field}}u_ih_i^2\sin\phi_i \\ \phi_i = \arctan\dfrac{y_i}{x_i}\ (0 \leqslant \phi_i \leqslant 2\pi) \end{cases} \tag{13}$$

where, $\xi_{\text{distortion}}$, ξ_{coma} and ξ_{field} are the weight coefficients of the actual lateral deviation of the stars on the image plane under the influence of distortion, coma and field curvature. $\kappa_{\text{distortion}}$, κ_{coma} and κ_{field} are distribution factors of distortion, coma and field curvature. u and h are object height and entrance pupil diameter.

The star position error correction model by the splicing star simulator can be established based on the aberration theory, as shown in Eq. (14).

$$\gamma' = \arctan\frac{\sqrt{\left[\left(x_m \pm \Delta X_m\right) - \left(x_n \pm \Delta X_n\right)\right]^2 + \left[\left(y_m \pm \Delta Y_m\right) - \left(y_n \pm \Delta Y_n\right)\right]^2}}{f} \tag{14}$$

where, γ' is the angular distance between M and N after the two star position error correction.

4 Experiment verification

To verify the accuracy of the star position error correction method of splicing star simulator based on lateral aberration, a star position error measurement device consisting of Leica theodolite, highprecision six-dimensional adjustment mechanism and multi-dimensional support was built to measure the star position error of the splicing star simulator, as shown in Fig.7.

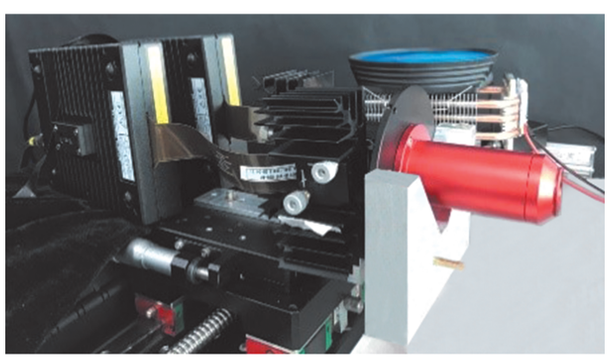

Fig.7 Measuring device of splicing star simulator

The correction formula of the star position error based on the lateral aberration was written in the star display and the control computer. Taking the orientation of the coordinate axis of the star sensor in the inertial coordinate system as an example, the navigation star that conforms to the star sensor pointing requirements was searched in the navigation star catalogue using the star display and the control computer, displayed on the LCOS, and emitted by the collimating optical system in the form of parallel light. The azimuth and pitch angle of the star were measured by the theodolite, and the theoretical angular distance between the central star andthe star to be measuredwas calculated according to Eq. (15).

$$\gamma_{\text{m}} = \arccos\left[\cos\beta_0\cos\beta_{\text{m}}\cos(\alpha_0 - \alpha_{\text{m}}) + \sin\beta_0\sin\beta_{\text{m}}\right] \tag{15}$$

where, (α_0, β_0) is the azimuth and pitch angle of the central star. (α_m, β_m) is the azimuth and pitch angle of the star to be measured. Table 2 lists the accuracies of the star simulator before and after correction.

Based on the analysis above, the position error of stars far away from the central star is relatively large and is seriously affected by aberration. It can be seen from the Fig.8 that the star position error basically increases with the increase of the theoretical angular distance between stars. The maximum uncorrected star position error is 48.78″, which cannot meet the technical requirements of the star simulator. According to the collimating optical system design of the splicing star simulator and lateral aberration analysis results, a correction formula for the star position error based on the lateral aberration was written in the star display and the control

computer, and the star map display and the star point position measurement were performed again. The test results show that the maximum star position error decreases to 10.75″, which meets the technical requirements of star simulator. The detailed test data before and after the correction of star position error are shown in Fig.8.

Table 2 Accuracies of the star simulator before and after correction

No.	α_m/(°)	β_m/(°)	Theoretical value/(°)	Error before correction/(″)	Error after correction/(″)
1	201.30	82.89	7.87	30.69	5.39
2	195.71	80.67	9.70	41.71	8.49
3	192.43	87.12	6.38	20.42	2.49
4	191.26	83.78	9.29	38.09	7.16
5	190.44	82.40	10.84	48.78	6.19
6	204.86	90.16	6.85	22.67	10.75
7	202.99	97.67	9.17	36.22	4.49
8	202.78	94.62	6.64	21.25	8.65
9	201.67	99. 35	10.08	42.84	7.95
10	199.45	99.75	9.91	40.63	1.66
11	199.11	93.41	3.59	11.13	8.25
12	197.90	97.00	7.05	26.79	9.33
14	194.68	88.37	3.79	11.37	7.55

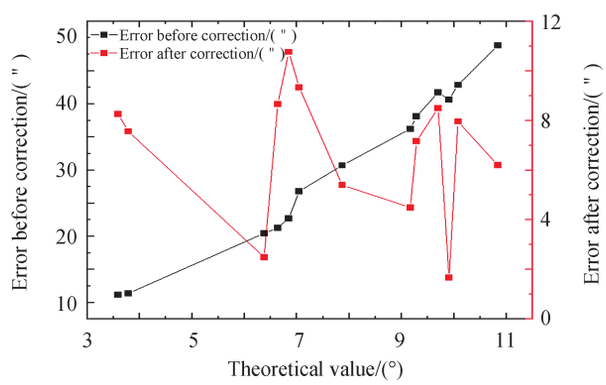

Fig.8 Variation of star position error before and after correction

5 Conclusion

This study proposed a method for correcting the star position error of splicing star simulator based on lateral aberration. The composition and working principle of splicing star simulator were introduced, and the main technical indicators and requirements were presented. The lateral aberration theory influencing imaging position and imaging quality of star point was analyzed and a small distortion flat field high imaging quality collimating optical system was designed by ZEMAX. Subsequently, combined with the working principle of the splicing star simulator, a measurement model of the star point position was established, and a star point position correction method based on the effects of distortion, coma, field curvature was proposed. This method can enhance the objectivity of the correction, through the analysis of the aberration of the optical system, the contribution of each aberration to the pixel offset is clarified. The comprehensive influence of the aberration is corrected, and the iterative focusing method can improve the starlight output accuracy of the system. A device for measuring star position error was built by utilizing the theodolite and six-dimensional adjustment mechanism. Experimental results demonstrate that the maximum uncorrected star position error is 48.78″, while the maximum corrected star position error is 10.75″, which meets the technical requirements of splicing star simulator. The splicing star simulator can be used for ground calibration and precision test of high precision star sensor.

References

[1] ZHANG Weina, QUAN Wei, GUO Lei. Blurred star image processing for star sensors under dynamic conditions[J]. Sensors, 2012, 12(5): 6712-6726.

[2] MCVITTIE G R,ENRIGHT J. Color star tracking I: star measurement[J]. Optical Engineering, 2012,51(8):084402.

[3] SUN Gaofei, MING Shanchi, ZHANG Guoyu, et al. Design of multi-magnitude star simulation system based on adjustable background[J]. Optik, 2020:164486.

[4] ZHANG Shuo, XING Fei, SUN Ting, et al. Novel approach to improve the attitude update rate of a star tracker[J]. Optics Express, 2018, 26(5):5164.

[5] WANG Mi, CHENG Yufeng, YANG Bo, et al. On-orbit calibration approach for optical navigation camera in deep space exploration[J]. Journal of Deep Space Exploration, 2016, 24(5):5536.

[6] FAN Chengcheng, WANG Mi, YANG Bo, et al. A method of high-precision ground processing for star sensor and gyro combination and accuracy verification[J]. Acta Optica Sinica, 2016, 36(11):1128002.

[7] SUN Ting, FEI Xing, WANG Xiaochu, et al. An accuracy measurement method for star trackers based on direct astronomic observation[J]. Scientific Reports, 2016, 6:22593.

[8] BOONE B G, BRUZZI J R, DELLINGER W F, et al. Optical simulator and testbed for spacecraft star tracker development[C].Proceedings of SPIE 5867,Optical Modeling and Performance Predictions II, 2005.

[9] WANG Lingyun, WANG Bo, ZHANG Guoyu, et al. Star point energy center correction method of star simulator[J]. Acta Photonica Sinica, 2016, 45(2): 153-158.

[10] MENG Yao. Study on key technique of high-precision dynamics star simulator based on LCOS splicing technology[D]. Changchun: Changchun University of Science and Technology,2016.

[11] XU Da, ZHANG Guoyu, SUN Gaofei. Design of star simulator with spatial background light[J]. Chinese Journal of Space Science, 2018, 38(4): 575-582.

[12] SUN Gaofei, ZHANG Guoyu, ZHENG Ru, et al. Star sensor calibration research and development[J]. Journal of Changchun University of Science and Technology, 2010, 33(4): 8-14.

[13] FENG Guangjun, MA Zhen, LI Yingcai. Design and performance analysis of standard starlight simulator[J]. Journal of Applied Optics, 2010, 31(1): 39-42.

[14] AN Yan, SUN Qiang, LIU Ying, et al. Design of astigmatism-free crossed Czerny-Turner spectrometer[J]. Optik-International Journal for Light and Electron Optics, 2013, 124(16):2539 - 2543.

[15] ZHANG Xiaojuan, ZHANG Guoyu, SUN Gaofei, et al. Spectral study for simulator on hybrid light source[J]. Acta Photonica Sinica, 2014, 43(2): 39-44.

[16] WANG Wensheng.Applied optics[M].Wuhan:Huazhong University of Science & Technology Press,2010.

[17] SUN Gaofei. Study on key technique of very high-precision star simulator[D]. Changchun: Changchun University of Science and Technology,2012.